Organometallic diphenols: The importance of the organometallic moiety on the expression of a cytotoxic effect on breast cancer cells

Elisabeth A. Hillard, Anne Vessières, Siden Top, Pascal Pigeon, Konrad Kowalski, Michel Huché, Gérard Jaouen

▶ **To cite this version:**

Elisabeth A. Hillard, Anne Vessières, Siden Top, Pascal Pigeon, Konrad Kowalski, et al.. Organometallic diphenols: The importance of the organometallic moiety on the expression of a cytotoxic effect on breast cancer cells. Journal of Organometallic Chemistry, 2007, 692 (6), pp.1315-1326. 10.1016/j.jorganchem.2006.10.041 . hal-01230402

HAL Id: hal-01230402
https://hal.science/hal-01230402

Submitted on 15 Mar 2024

HAL is a multi-disciplinary open access archive for the deposit and dissemination of scientific research documents, whether they are published or not. The documents may come from teaching and research institutions in France or abroad, or from public or private research centers.

L'archive ouverte pluridisciplinaire **HAL**, est destinée au dépôt et à la diffusion de documents scientifiques de niveau recherche, publiés ou non, émanant des établissements d'enseignement et de recherche français ou étrangers, des laboratoires publics ou privés.

Organometallic diphenols: The importance of the organometallic moiety on the expression of a cytotoxic effect on breast cancer cells

Elizabeth Hillard [a], Anne,* Vessières [a,*], Siden Top [a], Pascal Pigeon [a], Konrad Kowalski [b], Michel Huché [a], Gérard Jaouen [a,*]

[a] Laboratoire de Chimie et Biochimie des Complexes Moléculaires, UMR CNRS 7576, Ecole Nationale Supérieure de Chimie de Paris, 11, rue Pierre et Marie Curie, 75231 Paris Cedex 05, France

[b] Department of Chemistry, University Łódź, Narutowicza 68, 90-136 Łódź, Poland

Keywords: Bioorganometallic chemistry; Antitumor agents; Breast cancer; Metallocenes; Iron

Abstract

We have recently reported that the ferrocenyl diphenol compound 1,1-di(4-hydroxyphenyl)-2-ferrocenyl-but-1-ene **1** exhibited strong in vitro anti-proliferative effects on both hormone dependent (MCF7, IC_{50} = 0.7 μM) and hormone independent (MDA-MB231, IC_{50} = 0.6 μM) breast cancer cells. In order to assess the importance of the ferrocenyl motif, we have prepared a series of analogs using the organometallic fragments (η^5-C_5H_4)Cp*Fe (**7**), ((η^5-C_5H_4)$(CH_3)_2$phospholyl)Fe (**9**), (η^5-C_5H_4)CpRu (**10**), (η^5-C_5H_4)$Re(CO)_3$ (**11**), and (η^5-C_5H_4)$Mn(CO)_3$ (**12**), and the chlorinated ferrocenyl derivative 1,1-di(4-hydroxyphenyl)-2-ferrocenyl-4-chloro-but-1-ene (**4**). The nature of the organometallic moiety had a strong influence on estrogen receptor alpha (ERα) recognition, with relative binding affinity (RBA) values ranging from 0.55% to 10.8%. The second isoform of the estrogen receptor, ERβ, was better able to accommodate these compounds, with RBA values ranging from 8.9% to 17.1%. Molecular modeling studies suggest that the orientation of the compounds and their interactions with the residues of ERα and ERβ binding sites are very similar. A study on the MCF7 hormone dependent breast cancer cell line revealed an anti-proliferative effect for the ferrocenyl phenols **1** and **4**, while the other compounds displayed either a proliferative effect (**9**–**12**), or no effect (**7**). The anti-proliferative effect of **1** and **4** is also evident in the MDA-MB231 hormone independent breast cancer cell line (IC_{50}(**4**) = 1 μM), and can be attributed to the cytotoxicity of these compounds, while the other compounds showed no effect on this

cell line. The cytotoxicity of **1** and **4** may arise from electron delocalization in the radical cation in alkaline conditions, possibly resulting in a cytotoxic quinone methide formation, while the other complexes do not undergo the formation of this entity, as evidenced by the electrochemical results.

1. Introduction

Breast cancer treatment today commonly involves a lumpectomy, followed by a combination of endocrine therapy, radiotherapy and/or chemotherapy. The gold standard for endocrine therapy is the drug tamoxifen [1], whose hydroxylated metabolite inhibits cancer cell proliferation by competitively binding to the estrogen receptor (ER), although third generation aromatase inhibitors, which interfere with the production of estradiol have recently emerged as a superior treatment for post-menopausal women [2]. One important limitation of endocrine therapy is that it is only effective against patients with estrogen (and/or progesterone) receptor positive tumors. Patients with ER-negative (ER−), endocrine-resistant, invasive, or metastatic tumors are instead given a regimen of chemotherapeutic agents such as cyclophosphamide, doxorubicin, fluorouracil, and/or paclitaxel, which may give rise to adverse side effects because of their systemic cytotoxicity [2].

We have been exploring the creation of selectively cytotoxic molecules by the addition of putative cytotoxic moieties [3] in the form of metal cyclopentadienyls to the tamoxifen skeleton, a motif which has shown affinity for both isoforms (α and β) of the ER [4]. To this date, only in the case of the "hydroxyferrocifens", a series of compounds where a ferrocenyl group replaces the tamoxifen β-phenyl group, do the organometallic biovectors give rise to the desired combination of anti-estrogenic and cytotoxic activity [5]. By modifying various structural aspects of the hydroxyferrocifens, we have found that, in terms of pure cytotoxicity, one of the most efficacious compounds to date is the ferrocenyl diphenol compound **1** (Chart 1, 1,1-di(4-hydroxyphenyl)-2-ferrocenyl-but-1-ene). This compound shows high anti-proliferative activity in vitro against both hormone dependent (MCF7, IC_{50} = 0.7 μM) and independent (MDA-MB231, IC_{50} = 0.6 μM) breast cancer cell lines, as well as satisfactory relative binding affinities (RBAs) for both ER isoforms (ERα = 9.6%; ERβ = 16.3%) [6], and has become the standard to which we compare the activity of novel organometallic anti-cancer agents in our laboratory. We are currently studying the mechanism of action for compound **1**, and have recently posited an activation pathway which involves the in vitro oxidation of the ferrocene and phenol functionalities [7].

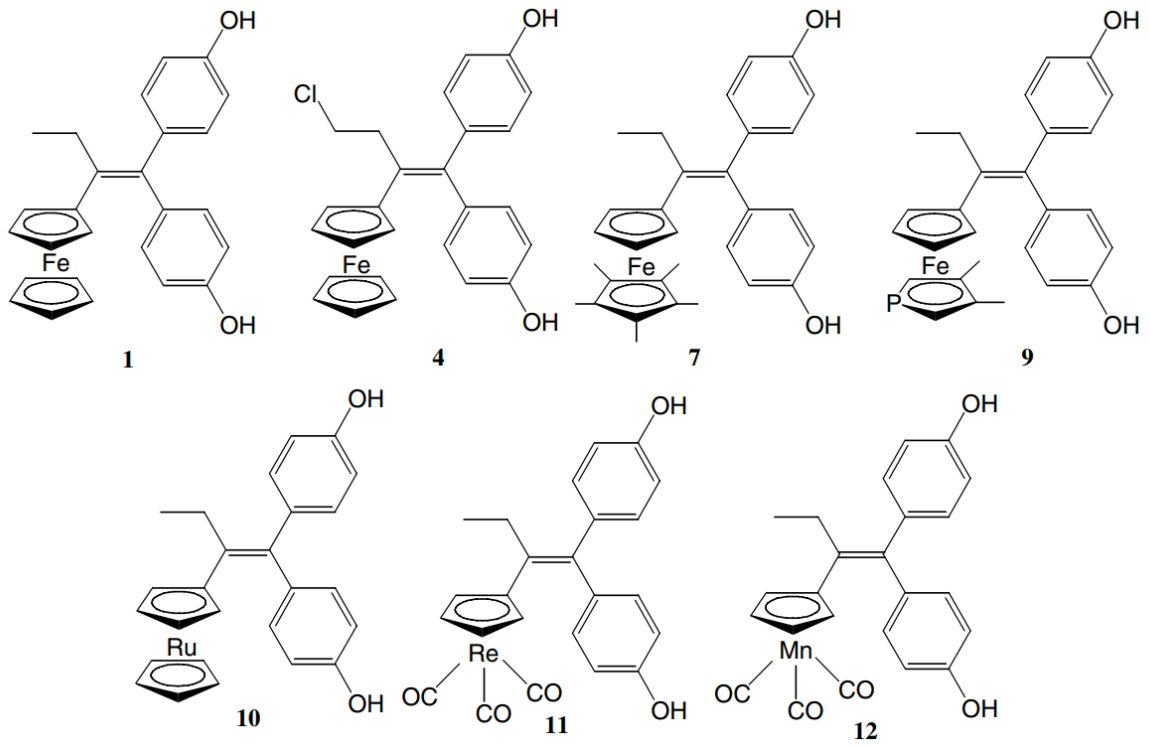

Chart 1. Organometallic diphenol compounds studied in this report.

The next logical step in our pursuit of compounds with greater cytotoxic efficacy and selectivity is to evaluate how the modification of the organometallic moiety influences the compounds' activity. To this end, we have created several diphenol analogs of **1**, shown in Chart 1, and tested their anti-proliferative activity against the ER positive MCF7 and ER negative MDA-MB231 breast cancer cell lines. We have tried to understand the biochemical results by investigating the molecules' oxidation chemistry by cyclic voltammetry, as well as their interactions with the ligand binding domain (LBD) of the estrogen receptor by molecular modeling calculations.

2. Results

2.1. Synthesis

The synthesis of **1** has been previously described [5], with a key step being a McMurry cross-coupling reaction between 4,4′-dihydroxybenzophenone and propionyl ferrocene. We have used this general strategy to further synthesize all of the diphenol compounds shown in Chart 1. For example, a Friedel–Crafts reaction of chloropropionyl chloride with ferrocene yielded

chloropropionylferrocene **3** which was then combined with 4,4′-dihydroxybenzophenone in the presence of $TiCl_4$ and Zn in refluxing THF to produce **4** in 48% yield (Scheme 1).

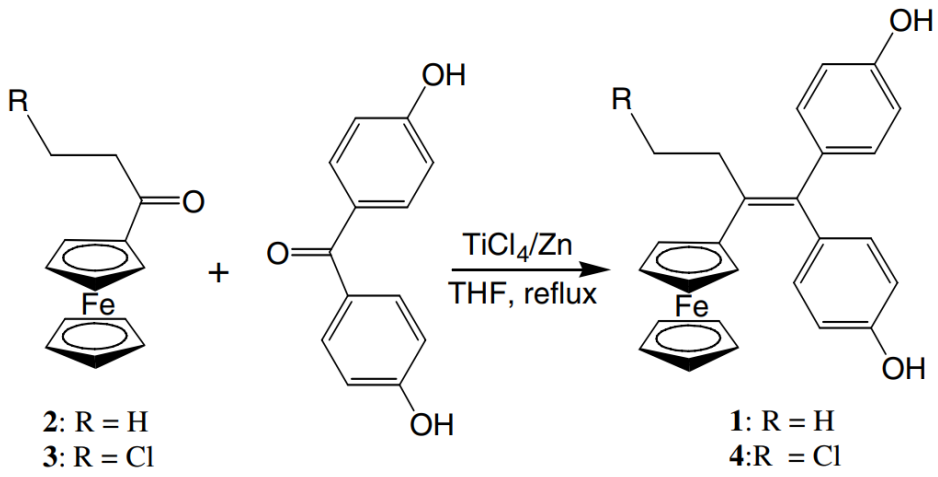

Scheme 1.

To obtain the permethylated derivative **7**, propionylferrocene **2** was heated in benzene in the presence of $AlCl_3$ [8], giving the propionylcyclopentadienyl benzene iron cation **5** in 70% yield. The reaction of lithium pentamethylcyclopentadienide with **5** in dimethyl ether produced ketone **6** in 13% yield, as shown in Scheme 2. Finally, the McMurry coupling between **6** and 4,4′-dihydroxybenzophenone gave compound **7** in 19% yield.

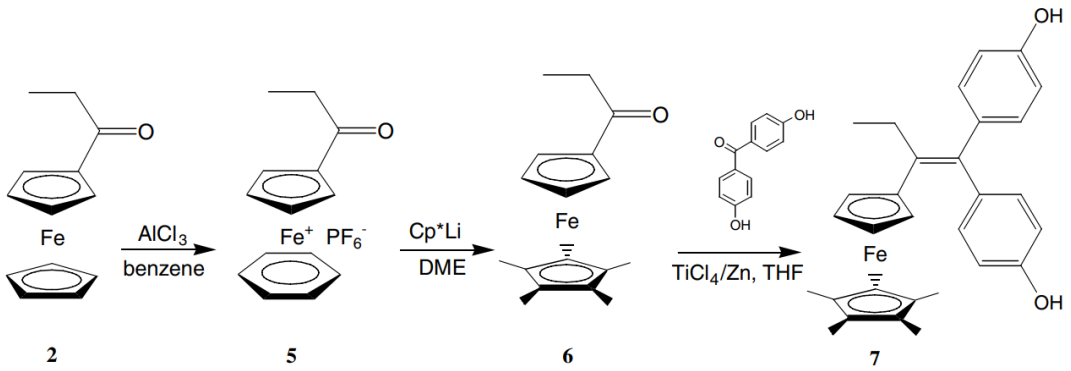

Scheme 2.

The phospholyl derivative **9** was synthesized similarly to the Cp^* derivative **7**. The ketone **8** was prepared by reacting dimethylphospholyl lithium with salt **5** in THF (Scheme 3), followed by a McMurry coupling between **8** and 4,4′-dihydroxybenzophenone, giving **9** in 16% yield. The syntheses of compounds **7** and **9** have been partially described in a preliminary communication [9].

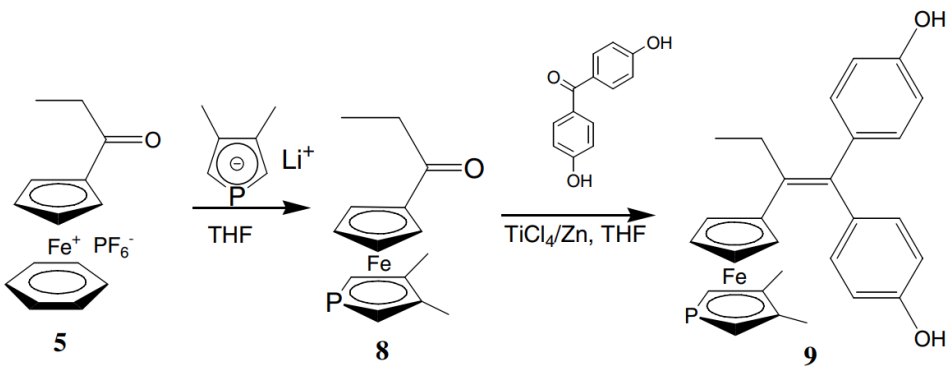

Scheme 3.

Compounds **10**–**12** were likewise synthesized via a McMurry reaction between the corresponding propionyl organometallic moieties, prepared by a Friedel–Crafts reaction of propionyl chloride with the corresponding metal cyclopentadienyl moiety as previously described [10] and 4,4′-dihydroxybenzophenone. In order to increase the yield of the cross-coupled product and reduce that of the expensive organometallic reagent self-coupled product, two equivalents of 4,4′-dihydroxybenzophenone were used. The yields calculated from the starting organometallic ketone were excellent (86–96%).

2.2. Biochemical results

2.2.1. RBA and lipophilicity values

The affinities for the estrogen receptor of the organometallic diphenols were measured on the two isoforms of the estrogen receptor, ERα and ERβ, and are reported as relative binding affinity (RBA) values in Table 1. The RBA of estradiol (E_2), the hormone of reference, is by definition 100%.

Table 1. Relative binding affinity (RBA) for ERα (cytosol) and ERβ (purified) and lipophilicity (log $P_{o/w}$) values of the diphenol complexes

Compound	**RBA (%)**[a]		**RBA Ratio (ERβ/ERα)**	**log $P_{o/w}$**
	ERα (cytosol)	**ERβ**		
Estradiol	100	100	1	3.3
1[b]	9.6 ± 1	16.3 ± 1.5	1.7	5.0
4	8.3 ± 0.3	10.8 ± 1.6	1.3	5.1
7	0.55 ± 0.5	8.9 ± 1.3	16.2	6.3
9	1.5 ± 0.4	10.8 ± 1.5	7.2	6.0
10	10.8 ± 0.6	17.1 ± 1.2	1.6	5.0
11	1.9 ± 0.1	11.1 ± 0.2	5.8	5.6
12	2.4 ± 0.2	13.0 ± 3.0	5.4	5.5

[a] Mean of two experiments ± range.

[b] Values from Ref. [6].

The ability of the complexes to recognize ERα varied widely, falling into two groups, those with satisfactory (**1**, **4**, **10**) and those with marginal (**7**, **9**, **11**, **12**) recognition. The capability of the receptor to accommodate the complexes seems dependant on the size of the organometallic substituent. For example, the affinities of the ferrocenyl and ruthenocenyl diphenols **1**, **4** and **10** were comparable (RBA = 8.3–10.8%), while those found for the more encumbered piano-stool complexes **11** and **12** were significantly weaker (1.9% and 2.4%). The recognition for ERα was lower yet for the highly encumbered pentamethylferrocene (**7**) and dimethylphosphaferrocene (**9**) complexes (RBA = 0.55% and 1.5%). Conversely, the β form of the receptor seemed to more easily accomodate the sterically hindered substituents; the range of RBA values for ERβ is quite limited, between 8.9% and 17.1%. In every case, the RBA values for ERβ were superior to those obtained with ERα, with the ratio of RBA(ERβ)/RBA(ERα) ranging from 1.3 to 16.2. Finally, the lipophilicity values were equal or superior to that of the ferrocenyl diphenol **1**. The highest values were found for **7** and **9**, which possess methylated ligands.

2.2.2. Study of proliferative/anti-proliferative effects

The effect of these complexes at a concentration of 1×10^{-6} M was studied on hormone-dependent (MCF7) and hormone-independent (MDA-MB231) breast cancer cells; the results are displayed in Fig. 1. On the ER+ MCF7 cells the observed behavior of the complexes can be classified in three groups. (1) The dimethylphosphaferrocene, Ru, Re, and Mn diphenols **9**–**12**, gave rise to significant proliferative effects, (2) the pentamethylferrocenyl diphenol **7** showed no effect, and (3) the ferrocenyl diphenols **1** and **4** yielded anti-proliferative effects. The proliferative effects observed for complexes **9**–**12** are undoubtedly due to activation of the ER; this estrogenic effect has been observed with related diphenol compounds [11]. Although the compounds are not structurally analogous to estradiol, they are able to interact with the ER in a similar way, which will be discussed further in the molecular modeling section. It is interesting to note, however, that there was no correlation between the wide ranging RBA values and the intensity of the estrogenic effect. The estrogenic effect was essentially the same (75–85% of the effect observed with E_2), and it seems impossible to determine a threshold RBA value where estrogenicity begins to be detected. It is clear however that in these cases the organometallic entities seem to act as simple spectators which do not impart any ER-independent cytotoxicity. This is not the case for the ferrocenyl complexes **1** and **4** which have an anti-proliferative effect (high for **1**, and moderate for **4**). Because **1** and **4** are structurally similar to **9**–**12**, one might expect to observe a proliferative effect arising from ER activation. That an anti-proliferative effect is measured instead, suggests that these compounds possess ER-independent cytotoxicity. The lack of an estrogenic effect for compound **7** may be attributed to its very weak affinity for ERα. It should be noted that the terms “proliferation” and “anti-proliferation” refer to observed phenomena, while the terms “cytotoxic” and “(anti)-estrogenic” describe mechanisms of action.

On the MDA-MB231 cells, which do not possess the α form of the receptor, only the ferrocene complexes **1** and **4** showed an anti-proliferative effect, which confirms their ER-independent cytotoxicity implied in the MCF7 experiments. Like estradiol, the other complexes had no effect. Therefore, one can conclude that compounds **9**–**12** exert their influence on the MCF7 cell line through the ER.

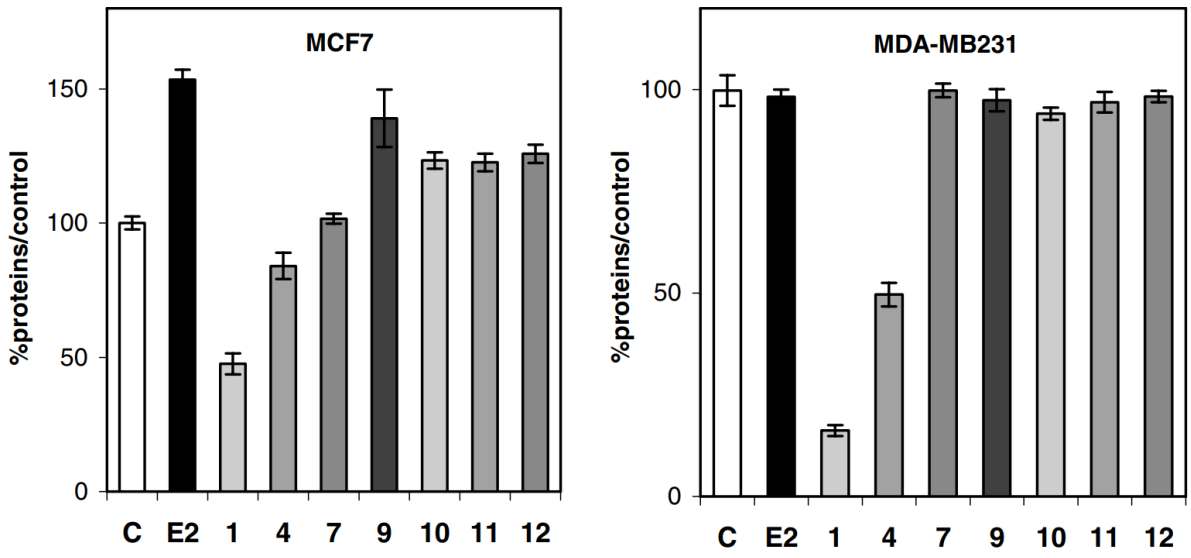

Fig. 1. Effect of 1 μM of the compounds and of 1 nM estradiol on the growth of MCF7 (hormone-dependent breast cancer cells, after 5 days of culture, medium with phenol red) and of MDA-MB231 (hormone-independent breast cancer cells, after 6 days of culture, medium without phenol red), C = control.

2.3. Molecular modeling

Molecular mechanics studies were performed to determine the conformation and, for compounds **1** and **4**, the stability of the ER–bioligand complex. The crystal structures of the ligand binding domain (LBD) of human ERα [12] with diethylstilbestrol (DES) or tamoxifen were used for the respective agonistic and antagonistic protein conformations, as well as the structure of ERβ occupied by (*R*,*R*)-5,11-*cis*-diethyl-5,6,11,12-tetrahydrochrysene-2,8-diol (agonist conformation) [13]. Only the amino acids forming the wall of the cavity were conserved and the native bioligands were digitally removed and replaced with the organometallic complexes. All the heavy atoms of the cavity were immobilized, except for the lateral chains of the amino acids His-524, Met-343, and Met-421 (for ERα) and His-475 (for ERβ), as these parts of the cavities have been shown to be flexible [14]. An energy minimization routine was carried out using the Merck Molecular Force Field (MMFF), to determine the best position for the bioligand under determination.

Fig. 2 represents the model of compound **1** docked in the LBD of ERα (2a) and ERβ (2b), and, for comparison, a hydroxyferrocifen molecule (where a $O(CH_2)_3N(CH_3)_2$ chain replaces one of the hydroxy groups in **1**) in the LBD of ERα (2c). In ERα, compound **1** showed an interaction of one of the phenol moities with Glu-353 and Arg-394 (and one interstitial water molecule) as schematically shown in Chart 2.

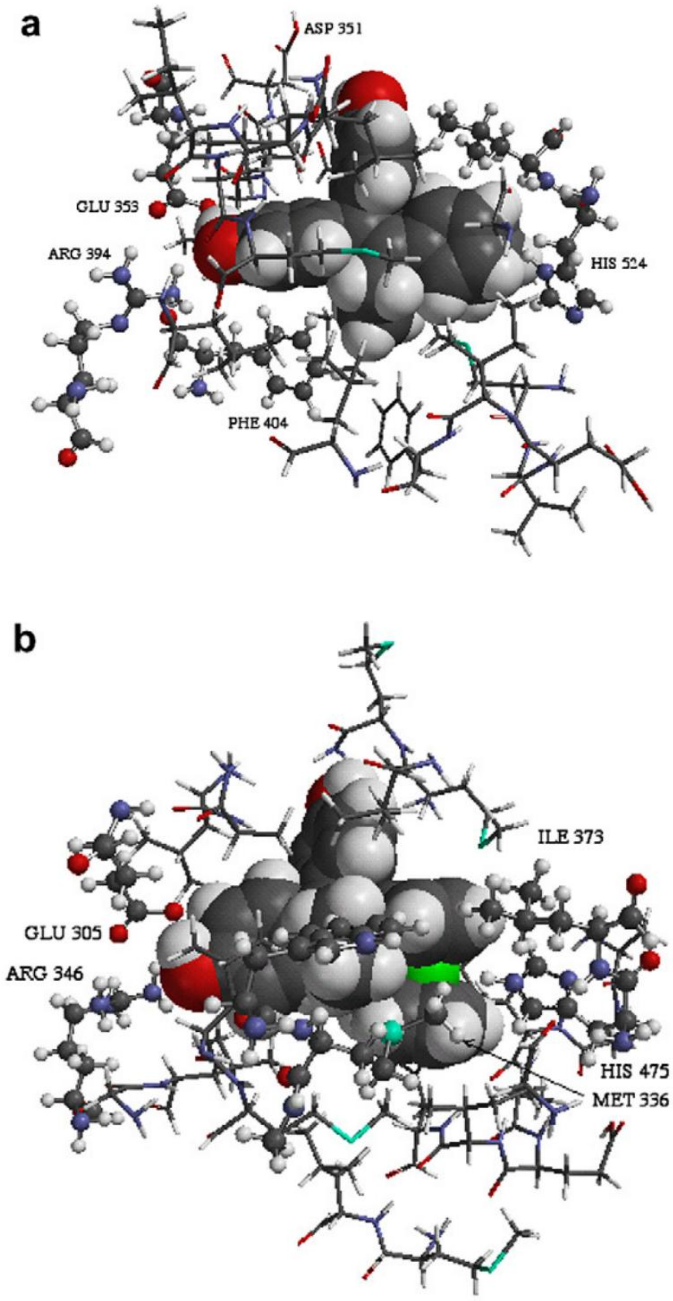
a
ASP 351
GLU 353
ARG 394
HIS 524
PHE 404
b
ILE 373
GLU 305
ARG 346
HIS 475
MET 336

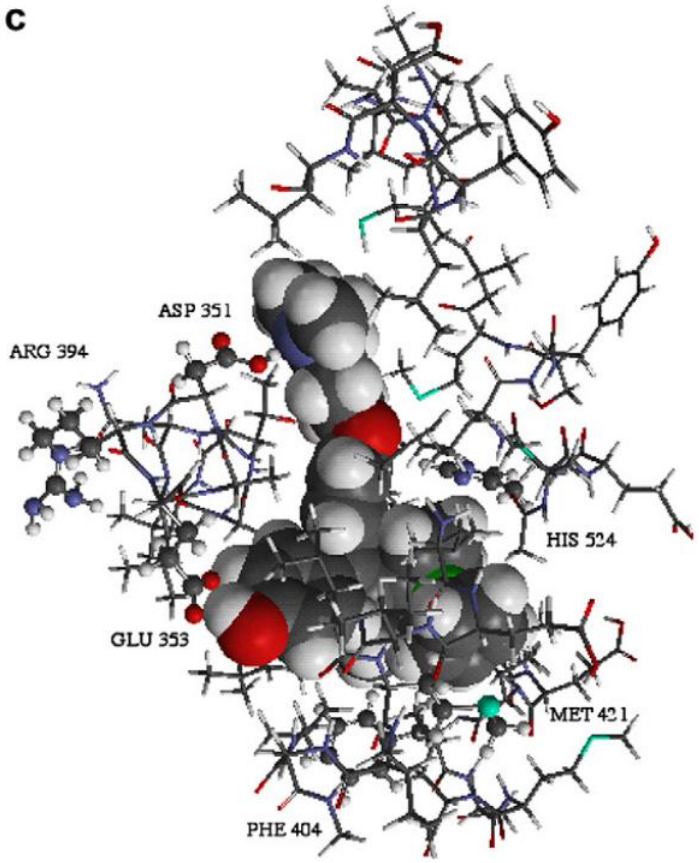

Fig. 2. Compound **1** in the LBD of (a) ERα (b) ERβ, and (c) OH-ferrocifen (n = 3) in ERα.

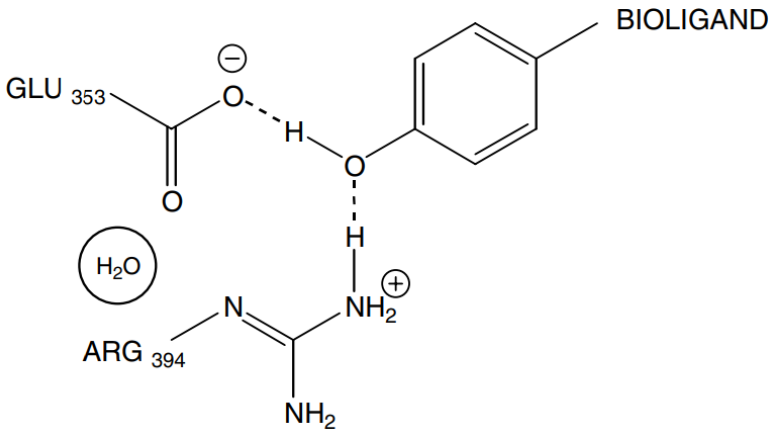

Chart 2.

At the opposite boundary of the LBD, the imidazole of His-524 formed a hydrogen bond with the ferrocenyl iron atom, with a hydrogen–iron bond distance of 2.9 Å, and a Mulliken charge on the iron atom of −0.214 as shown in Chart 3.

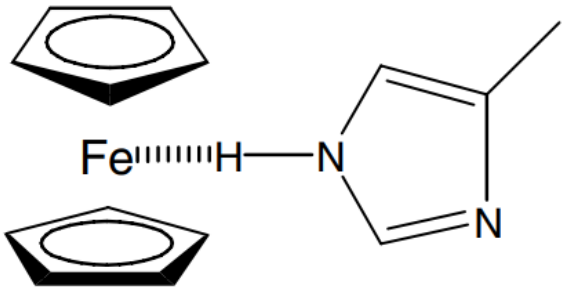

Chart 3.

Between these two hydrogen bonding associations at either extremity, the hydrophobic central portion of the molecule engaged in Van der Waals interactions with lipophilic residues.

The diagram of the association of **1** with ERβ is very similar to that of ERα: the phenol group associates with residues Glu-305 and Arg-346, and the ferrocene with His-475. The residues of the amino acids between the two polar association sites are different from those in the LBD of ERα but also engage in lipophilic van der Waals associations with the carbon skeleton of **1**. The same situation applies to compound **4**, which carries a $–CH_2–CH_2–Cl$ chain, instead of $–CH_2–CH_3$.

Compound **1** has been predicted to act as an estrogen with respect to ERα in MCF7 cells [6], although any estrogenic effect was masked by a strong ER-independent cytotoxic effect, giving rise to an overall observed anti-proliferative effect. On the other hand, the hydroxyferrocifens, which possess an amino chain, gave rise to an anti-estrogenic effect [5], in combination with an ER-independent cytotoxic effect. The differences in conformation of ERα for compound **1** and the hydroxyferrocifens can be observed in Fig. 2. It is seen in Fig. 2c that the steric effect of the basic chain changes the position of helix 12 of the LBD and that one observes a stabilizing interaction between Asp-351 and the chain nitrogen atom. This is similar to the interaction of hydroxytamoxifen with the LBD, as observed from crystallographic studies [12]. This conformation, however, cannot be obtained with **1** in ERα, because the second phenol group is situated too distant from Asp-351. Thus, the mode of association is agonistic in nature. This is also the case for diphenol compounds **4**, **7**, and **9**–**12** (data not shown).

2.4. Electrochemical results

Variable scan rate cyclic voltammograms were obtained using a platinum working electrode and saturated calomel reference electrode in methanol and methanol/pyridine (6:1, v:v) solutions; unfortunately, the insolubility of these compounds precluded their study in aqueous solution. The compounds exhibited a diversity of electrochemical behavior; that of the cytotoxic compounds **1** and **4** will be most fully addressed presently [15]. In methanol, compounds **1** and **4** gave rise to an apparently reversible one-electron Fc/Fc^{+} couple, as well as a higher potential irreversible phenol oxidation wave. Alternatively, in the presence of pyridine, the ferrocene electro-oxidation was irreversible, and the phenol oxidation wave underwent a cathodic shift, indicating a chemical reaction between the electrochemically generated cation and pyridine. Furthermore, the enhancement of the ferrocene oxidation wave in the presence of pyridine suggests the chemical regeneration of the Fe(II) species on the electrochemical timescale, Fig. 3a.

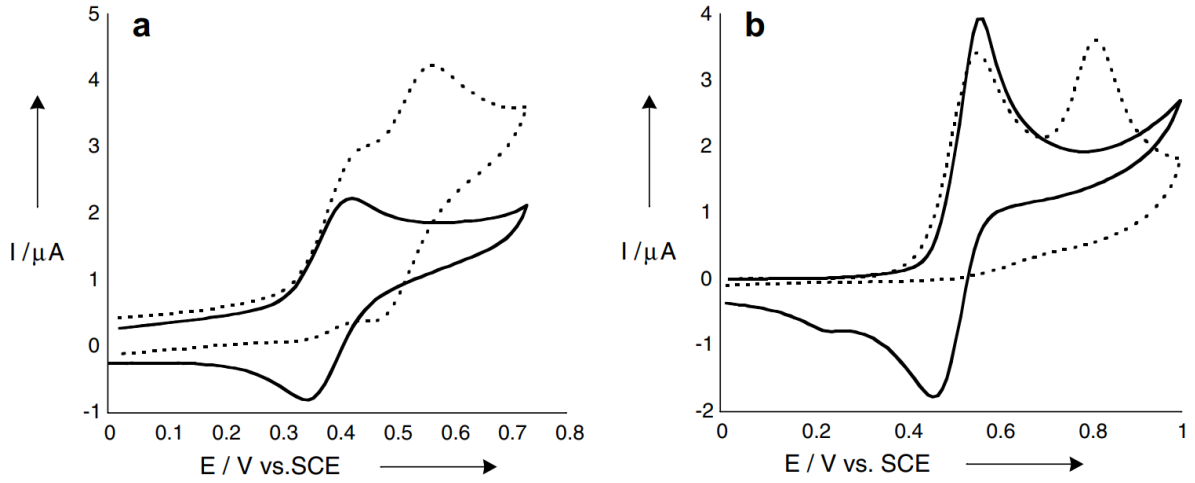

Fig. 3. Cyclic voltammograms vs. SCE for (a) **4** and (b) **10** in MeOH (solid line) and MeOH/py (dashed line). Scan rate = 0.5 V/s, platinum working electrode of 0.5 mm. Intensities have been normalized for concentration of compound. For compound **4**, irreversible higher potential waves were observed at 0.873 V (MeOH) and 0.584 and 0.837 V (MeOH/py).

This particular electrochemical signature was not observed for the non-cytotoxic compounds. Their electrochemical behavior is diverse, and for most of the compounds (except **7**), a fast chemical reaction seems to follow electro-oxidation. For the ruthenocene compound **10**, the electrochemical behavior was especially complex. At low scan rates, the oxidation wave *appeared* reversible, but the reduction wave rapidly disappeared with increasing scan

rate, suggesting follow-up chemistry involving the cation. It should be noted that the reversible oxidation of ruthenocene has only been previously observed with weakly coordinating anions in non-protic solvents [16]. In the presence of pyridine, two irreversible oxidation waves were observed, the first metal centered, and the second phenol centered, and no regeneration of the Ru(II) species was observed, Fig. 3b.

Compound **7** gave rise to a low potential apparently reversible Fc/Fc+ couple both in methanolic and methanol/pyridine solutions, indicating that the cation radical remains ferrocene-centered and stable on the electrochemical timescale, probably due to the electron donating properties of the methylated Cp^*. The CVs of compounds **11** and **12** were also unchanged by the addition of pyridine; their oxidation waves were irreversible up to 20 V/s in both methanol and methanol/pyridine. Comparison of the oxidation potentials of **11** and **12** with those of $CpRe(CO)_3$ and $CpMn(CO)_3$, suggest that the first wave arises from a metal centered oxidation, while the second oxidation wave likely arises from a phenol centered oxidation. This interpretation is supported by the observation that the second oxidation wave of **11** and **12** caused immediate passivation of the electrode, a common problem with anodic reactions of phenols [17]. Oxidation potentials are given in Table 2.

Table 2. Oxidation potentials vs. SCE in MeOH and MeOH/py (6:1)

Empty Cell	**Solvent**	***E*(1)/V**	***E*(2)/V**
1	MeOH	0.373(2)	0.88(3)[a]
	MeOH/py	0.387(3)	0.480(2)[a]
4	MeOH	0.413(2)	0.87(4)[a]
	MeOH/py	0.460(2)	0.584(3)[a]
7	MeOH	0.153(3)	Not observed
	MeOH/py	0.171(2)	0.83(4)[a]
10	MeOH	0.564(2)	Not observed
	MeOH/py	0.553(3)[a]	0.811(3)[a]
11	MeOH	0.880(3)[a]	Absorption

Empty Cell	**Solvent**	***E*(1)/V**	***E*(2)/V**
	MeOH/py	0.866(4)[a]	Absorption
12	MeOH	0.838(3)[a]	Absorption
	MeOH/py	0.829(4)[a]	Absorption

Scan rate = 0.5 V/s, 0.5 mm Pt electrode.

[a] Irreversible.

3. Discussion

The proliferative/anti-proliferative effects on the ER+ MCF7 cell line are primarily hormone dependent, and therefore controlled by the interaction of the complexes with the ligand binding domain of the estrogen receptor. For tamoxifen, the anti-estrogenic effect is due to the long amine chain which prevents helix 12 from folding onto helix 4, causing the ER to adopt an "open" conformation which is inimical to the binding of the necessary coactivators for DNA transcription. However, the compounds in this study do not possess this chain and thus would be predicted to have a proliferative effect on the MCF7 breast cancer cell line. This is indeed what is observed for compounds **9**–**12**. Compound **7** shows essentially no effect, and this can be attributed to the very low affinity of this compound for ERα, probably due to the bulkiness arising from the methylated Cp ring. Compounds **1** and **4**, on the other hand, show an unexpected anti-proliferative effect. Given the structure of these compounds and the results of the molecular modeling studies, this effect can only be attributed to the inherent cytotoxicity of the compounds. This interpretation is supported by the study on the ER negative MDA-MB231 cell line, where compounds **7**, **9**–**12** show no effect and compounds **1** and **4** show an anti-proliferative effect.

While estrogenic effects are governed by specific interactions of the bioligand with the ER, cytotoxicity is a more general phenomenon, and may arise from a number of biochemical interactions and pathways. Cytotoxicity with respect to ferrocenyl compounds has previously been attributed to oxidation to the ferrocenium cation, which can then engage in Fenton generation of highly reactive hydroxyl radicals [18]. However, the most active compound in the study of Tabbi et al., decamethyl-ferrocenium tetrafluoroborate, yielded an IC_{50} value of 35 μM in the MDF7 cell line. Our electrochemical studies, as well as the observation that compound **1** is more than an order of magnitude more active against the MCF7 cell line, has

led us to recently propose an alternative mechanism, involving the pH-dependent in vitro generation of reactive quinone methides (QMs), mediated by initial ferrocene oxidation by ROS in the cell [7]. Bolton and coworkers have shown that hydroxytamoxifen and its chlorinated derivative, hydroxytoremifene, can yield QMs after treatment with chemical (MnO_2) and biochemical (cytochrome P450) oxidants, and the QMs have been shown to form adducts with glutathione (GSH) [19]. However, no QM–GSH adducts were detected in MCF7 cells incubated with hydroxytamoxifen or hydroxytoremifene, suggesting that QMs cannot be formed from these compounds in the absence of oxidizing enzymes.

The electrochemical results for the cytotoxic ferrocene compounds **1** and **4** have been previously reported [7], and can be summarized as follows. In the presence of methanol, a reversible ferrocene/ferrocenium couple is observed, with higher potential waves arising from irreversible phenol oxidation. However, when an organic base is added (pyridine), the ferrocenium reduction wave is lost, due to intramolecular electron transfer from the phenol moiety to the ferrocenium radical cation coupled with proton abstraction. The loss of a second (net) hydrogen atom from the α-carbon of the ethyl group may result in a QM structure for compounds **1** and **4** [7]. Because the potentials necessary to form the ferrocenyl QM are considerably lower than the first oxidation potential of tamoxifen (approximately 0.8 V vs. SCE in our system), it can be postulated that this transformation can occur in vitro in mild conditions, instead of requiring cytochrome P450 enzymes.

All of the diphenol compounds discussed in this report could theoretically form QMs under oxidizing conditions, and a study of the relationship between their electrochemical reactivity with their biological effects was pursued. The diversity of their electrochemical behavior, however, makes it impossible to offer any correlation, except to remark that only in the case of the ferrocene compounds did the electrochemical behavior suggest QM formation. The radical cations of **10**–**12** are extremely unstable; indeed, the efforts to generate stable 17-electron ruthenium and $[CpM(CO)_3]^+$ species have been considerable, and have only recently been successful by the use of weakly coordinating anion electrolytes [16], [20]. On the other hand, although compound **7** did give rise to a reversible one electron metal centered redox couple, it did not display any intramolecular electron transfer behavior, and showed no reactivity with pyridine whatsoever. Finally, although the CV of **10** changed dramatically upon the addition of pyridine, there was no chemical regeneration of **10** from $\mathbf{10}^+$, as evidenced by the lack of enhancement of the oxidation wave. Therefore, to summarize, of all the tested compounds, only the cytotoxic molecules **1** and **4** had a particular electrochemical signature which strongly suggests the formation of a QM structure as a cytotoxic agent.

It is interesting to note that compound **1** is significantly more cytotoxic than compound **4**, with IC_{50} values for ER− MDA-MB231 breast cancer cells of 0.6 and 1 μM, respectively. This is surprising, in that the β-Cl substitution on **4** would be expected to acidify the α-H, leading to easier QM formation. However, if for compounds **1** and **4**, QM formation is indeed mediated by initial ferrocene oxidation, the influence of the chloro group may be less important on the α-H than it is on the ferrocene oxidation potential. The chloro substituent shifts the ferrocene oxidation of **4** by +40 mV in MeOH and +73 mV in MeOH/py compared to **1**, which may account for the somewhat lower efficacy of **4**.

4. Conclusions and prospects

We have reported the synthesis and proliferative/anti-proliferative effects of a series of organometallic diphenol butene compounds. In the ER+ breast cancer cell line, all of the compounds gave rise to cell proliferation, except for the ferrocenyl compounds **1** and **4**, which displayed a strong anti-proliferative effect. Likewise, only these compounds engendered an anti-proliferative effect on the ER– breast cancer cell line. The latter observation, coupled with molecular modeling studies, implies that all of the compounds (except **7**) are estrogenic, and that **1** and **4** additionally possess a strong cytotoxic activity. Electrochemical studies suggest that this cytotoxicity arises from the formation of QMs via oxidative intercellular metabolism. Nothing is known about the in vitro behavior of compounds **1** and **4** at this stage, except that the compounds have a good affinity for both isoforms of the ER. However, some interesting recent research suggests some promising new directions. In serum-free medium, tamoxifen and toremifene have been shown to cause rapid, non-genomic in vitro cancer cell death, which is associated with the elevation of oxidative stress via a mitochondrial pathway that involves NADPH oxidase [21]. It is also known that natural phenols such as caffeic and ferulic acid exert their protective and anti-cancer effects via the NADPH oxidase [22]. This could therefore constitute a possible target accounting for the observed cytotoxic effects of **1** and **4**, and will be the subject of a later study.

This oxidative mechanism is quite a new paradigm in the use of metals in medicine. Currently, due to the excellent success of cisplatin in the treatment of testicular cancer, the focus has predominantly been on the synthesis of DNA alkylating agents, which are activated by ligand hydrolysis. For example, the study of platinum pharmaceuticals continues apace [23], and several ruthenium “piano stool” compounds have been shown to bind to DNA after hydrolysis of a halogen ligand [24].

However, new strategies are currently being developed. For example, the Ru complex KP1019 (indazolium *trans*-[tetrachlorobisindazole-ruthenate(III)]), currently in Phase II trials, induces apoptosis and DNA strand-breaks in colorectal cancer cells and is activated by reduction of the Ru(III) atom [25]. The anti-tumor compounds gallium maltolate (tris(3-hydroxy-2-methyl-4*H*-pyran-4-onato)gallium(III)) and KP46 (tris(8-quinolinolato)gallium(III)), also in Phase I clinical trials, cause cell death by mimicking iron and interfering with the iron-dependent ribonucleotide reductase enzyme [26]. The Ru complex NAMI-A (imidazolium-*trans*-tetrachloro(dimethylsulfoxide) imidazoleruthenium(III)) [27] which has completed Phase I trials, inhibits the spontaneous generation of lung metastases, but is not cytotoxic towards the primary tumor, while RAPTA compounds ($RuCl_2(\eta^6$-arene)(1,3,5-triaza-7-phosphaadamantante) have recently also been found to show anti-metastatic activity [28]. Put into this perspective, the ability of the ferrocene group to act synergistically with phenol functionalities is but another pathway to cell death. However, in the fight against a disease as multifaceted as cancer, it is unlikely that one "magic bullet" will be found, and an arsenal of organometallic compounds which exhibit cytotoxicity via a host of different mechanisms may have a promising future as agents in multi-acting drug cocktails.

5. Experimental

5.1. General remarks

The synthesis of all compounds was performed under an argon atmosphere, using standard Schlenk techniques. Anhydrous THF and diethyl ether were obtained by distillation from sodium/benzophenone. TLC chromatography was performed on silica gel 60 GF254. Infrared spectra were obtained on an IRFT BOMEM Michelson-100 spectrometer equipped with a DTGS detector. ^{1}H and ^{13}C NMR spectra were recorded on Bruker spectrometers. Mass spectra were obtained on a Nermag R 10-10C spectrometer. High resolution mass spectrometry (HRMS) was performed on a JEOL MS 700 instrument. Melting points were measured with a Kofler device. Elemental analyses were performed by the microanalysis services of Pierre et Marie Curie University (Paris, France) or of ICSN (Gif sur Yvette, France). Molecular modeling studies were carried out utilizing Mac Spartan Pro, PC Spartan Pro, Odyssey, and Titan [29].

5.2. Synthesis

The syntheses and characterization of **1** and **2** has been previously described in a report from our laboratory [5]. 3-Chloropropionyl-ferrocene, **3**, has been reported in the literature [30].

5.2.1. 1,1-Di(4-hydroxyphenyl)-2-ferrocenyl-4-chloro-but-1-ene (**4**)

$TiCl_4$ (3.3 ml, 30 mmol) was added dropwise to a suspension of zinc powder (3.5 g, 54 mmol) in 50 ml of THF at −10 °C. The dark grey mixture obtained was heated at reflux for 1.5 h. A solution of THF (10 ml) containing 4,4′-dihydroxybenzophenone (1.2 g, 5.6 mmol) and ketone **3** (1.3 g, 4.8 mmol) was added dropwise to the first solution and then the resulting mixture was heated for 2 h. After cooling to room temperature, the mixture was hydrolyzed with 20% HCl solution. After CH_2Cl_2 extraction and solvent removal, the crude product was chromatographed on silica gel column with CH_2Cl_2/acetone 10:1 as eluent to yield **4** as an orange solid (0.45 g, 47% yield, mp 114 °C). ^{1}H NMR (400 MHz, acetone-d_6): δ 3.18 (t, J = 8.1 Hz, 2H, CH_2), 3.61 (t, J = 8.1 Hz, 2H, CH_2Cl), 3.99 (t, J = 1.9 Hz, 2H, C_5H_4), 4.16 (t, J = 1.9 Hz, 2H, C_5H_4), 4.21 (s, 5H, Cp), 6.74 (d, J = 8.7 Hz, 2H, C_6H_4), 6.89 (d, J = 8.7 Hz, 2H, C_6H_4), 6.90 (d, J = 8.7 Hz, 2H, C_6H_4), 7.14 (d, J = 8.7 Hz, 2H, C_6H_4), 8.31 (s, 1H, OH), 8.40 (s, 1H, OH). ^{13}C NMR (100 MHz, acetone-d_6): δ 39.9 (CH_2), 45.2 (CH_2Cl), 69.7 (2CH, C_5H_4), 70.6 (5CH, Cp), 70.7 (2CH, C_5H_4), 88.8 (C, C_5H_4), 116.5 ($2CH_{arom}$), 116.9 ($2CH_{arom}$), 131.9 ($2CH_{arom}$), 132.5 ($2CH_{arom}$), 137.0 (C) 137.5 (C), 142.5 (2C), 157.7 (C), 157.8 (C). IR (KBr): 3438 (OH), 3093, 3031, 2958 (CH_2) cm^{-1}. HRMS (EI): m/z: [$C_{26}H_{23}{}^{35}ClFeO_2$: M^+] calcd: 458.0737, found: 458.0737, [$C_{26}H_{23}{}^{37}ClFeO_2$] calcd: 460.0720, found: 460.0716. Anal. Calc. for $C_{26}H_{23}ClFeO_2$: C, 68.07; H, 5.05. Found: C, 67.79; H, 5.54%.

5.2.2. Propionylcyclopentadienyl-benzene-iron hexafluorophosphate (**5**)

Propionylferrocene **2** (3.8 g, 15.7 mmol) was dissolved in 25 ml of benzene. To this solution was added $AlCl_3$ (8.5 g, 64.4 mmol). The mixture was heated under reflux for 2.5 h. After cooling to room temperature a dark blue solid was formed on the flask bottom. The red brown solution was eliminated by decantation. Iced water was added to the solid, forming a yellow green solution. This aqueous solution was washed with diethyl ether until the organic phase became colorless. A solution of ammonium hexafluorophosphate was added to the yellow solution in small portions. A yellow solid precipitated from the mixture. This addition was stopped when no more precipitate was formed. The yellow solid obtained was collected by filtration, washed by water followed by diethyl ether, and dried under vacuum to yield **5** (4.0 g, 70 % yield). ^{1}H NMR (400 MHz, acetone-d_6): δ 1.14 (t, 3H, J = 6.8 Hz, CH_3), 3.02 (q, 2H, J = 6.8 Hz, CH_2), 5.46 (broad s, 2H, C_5H_4), 5.74 (broad s, 2H, C_5H_4), 6.53 (s, 6H,

C_6H_6). ^{13}C NMR (100 MHz, acetone-d_6): δ 7.56 (CH_3), 34.4 (CH_2), 79.7 (2CH, C_5H_4), 76.9 (2CH, C_5H_4), 86.1 (C, C_5H_4), 90.3 (6CH, C_6H_6), 201.1 (CO). IR (KBr) 1693 (CO) cm^{-1}. Anal. Calc. for $C_{14}H_{15}F_6FeOP$: C, 42.03; H, 3.78. Found: C, 42.12; H, 3.63%.

5.2.3. Propionylcyclopentadienyl-pentamethylcyclopentadienyl-iron (**6**)

In a Schlenk tube, pentamethylcyclopentadiene (0.82 g, 6.0 mmol) was dissolved in 17 ml of diethyl ether. The solution was heated to 50 °C and a 2.5 M solution of *n*-BuLi in hexane (6.4 mmol, 2.6 ml) was slowly added dropwise. A white precipitate of the Li salt appeared. After 15 min of stirring, propionylcyclopentadienyl-benzene-iron hexafluorophosphate **5** (1.0 g, 2.5 mmol) was added in one portion. The solution became red. After stirring at 50°C, the mixture was poured into water. The product was then extracted with CH_2Cl_2. The organic phase was dried over $MgSO_4$, filtered and evaporated. The crude product obtained was chromatographed on silica gel column by using CH_2Cl_2 as eluent to yield **6** as a red solid (0.25 g, 13% yield, mp 80 °C). ^1H NMR (400 MHz, $CDCl_3$): δ 1.16 (t, 3H, J = 7.3 Hz, CH_3), 1.80 (s, 15H, CH_3 from Cp*), 2.60 (q, 2H, J = 7.3 Hz, CH_2), 4.02 (t, 2H J = 1.9 Hz, C_5H_4), 4.26 (t, 2H J = 1.9 Hz, C_5H_4). ^{13}C NMR (50 MHz, $CDCl_3$): δ 8.0 (CH_3), 10.4 (5CH_3, Cp*), 32.8 (CH_2), 71.5 (2CH, C_5H_4), 76.0 (2CH, C_5H_4), 80.2 (C, C_5H_4), 81.3 (5C, Cp*), 203.8 (CO). MS (70 eV, EI): *m/z*: 312 [M^+], 283 [$M-C_2H_5^+$], 255 [$M-COC_2H_5$+]. IR (KBr): 1656 (CO) cm^{-1}. Anal. Calc. for $C_{18}H_{24}FeO$: C, 69.24; H, 7.75. Found: C, 69.08; H, 7.77%.

5.2.4. 1,1-Di(4-hydroxyphenyl)-2-pentamethylferrocenyl-but-1-ene (**7**)

$TiCl_4$ (3.0 ml, 27.3 mmol) was added dropwise to a suspension of zinc powder (2.5 g, 38.4 mmol) in 20 ml of THF at −10 °C. The dark grey mixture obtained was heated at reflux for 1.5 h. A solution of THF (10 ml) containing 4,4'-dihydroxybenzophenone (0.55 g, 2.5 mmol) and ketone **6** (0.40 g, 1.2 mmol) was added dropwise to the first solution and the resulting mixture was heated for 2 h. After cooling to room temperature, the mixture was hydrolyzed with 20% HCl solution. After CH_2Cl_2 extraction and solvent removal, the crude product was chromatographed on silica gel column with CH_2Cl_2/acetone 10:1 as eluent to yield **7** as an orange solid (0.11 g, 19% yield, mp 159°C). ^1H NMR (400 MHz, CD_2Cl_2): δ 0.94 (t, 3 H, J = 7.2 Hz, CH_3), 1.52 (s, 15H, CH_3), 2.16 (broad q, 2H, J = 7.2 Hz, CH_2), 3.55 (s, 2H, C_5H_4), 3.73 (s, 2H, C_5H_4), 5.00 (very broad s, 2H, OH), 6.76–6.72 (m, 4H, C_6H_4), 6.92 (d, 2H, J = 8 Hz, C_6H_4), 7.02 (d, 2H, J = 8 Hz, C_6H_4). ^{13}C NMR (100 MHz, CD_2Cl_2): δ 10.3 (5CH_3), 14.7 (CH_3), 26.2 (CH_2), 71.3 (2CH, C_5H_4), 71.7 (5C, Cp*), 73.4 (2CH, C_5H_4), 87.8 (C, C_5H_4), 114.6 ($2CH_{arom}$), 114.8 ($2CH_{arom}$), 130.2 ($2CH_{arom}$), 130.6 ($2CH_{arom}$), 130.9 (C), 135.9 (C), 153.6 (C), 137.0 (C), 137.6 (C), 153.8 (C). IR (KBr): 3414

(OH), 1606 (C=C) cm^{-1}. HRMS (CI): *m/z*: [$C_{31}H_{35}FeO_2$: MH^+] calcd: 495.1987, found: 495.1976.

5.2.5. Propionylcyclopentadienyl-(3,4-dimethylphospholyl)-iron (**8**)

In a Schlenk tube, 3,4-dimethylphosphole (1.32 g, 7.0 mmol) was dissolved in 50 ml of THF. Lithium (0.15 g, 21.0 mmol) cut in small pieces was added in the solution. The mixture was stirred for 2.5 h at room temperature. The dark mixture was cannulated to another Schlenk tube, leaving behind the unreacted lithium. Propionylcyclopentadienyl-benzene-iron hexafluorophosphate (**6**) (3.31 g, 8.27 mmol) was added to the mixture in one portion. The solution became red. After stirring at 50 °C for 30 min, the mixture was poured in water. The product was then extracted with CH_2Cl_2. The organic phase was dried over $MgSO_4$, filtrated and evaporated. The crude product obtained was chromatographed on silica gel column by using CH_2Cl_2 as eluent to yield **8** as a red solid (0.45 g, 22% yield). ^{1}H NMR (400 MHz, $CDCl_3$): δ 1.16 (t, 3H, J = 7.2 Hz, CH_3), 2.10 (s, 6H, CH_3), 2.71 (q, 2H, J = 7.2 Hz, CH_2), 3.73 (d, 2H, $J_{P–H}$ = 36 Hz, C_4H_2P), 4.42 (t, 2H, J = 1.8 Hz, C_5H_4), 4.78 (t, 2H, J = 1.8 Hz, C_5H_4). ^{13}C NMR (100 MHz, $CDCl_3$): δ 8.2 (CH_3), 15.5 ($2CH_3$), 33.1 (CH_2), 72.3 (2CH, C_5H_4), 75.1 (2CH, C_5H_4), 81.0 (d, $^2J_{P–C}$= 47.5 Hz, C_4H_2P), 81.2 (C, C_5H_4), 96.3 (d, $^2J_{P–C}$ = 7.1 Hz, C_4H_2P), 204.0 (CO). ^{31}P NMR (161.9 MHz, $CDCl_3$): δ 77.5 (d, $^2J_{P–H}$ = 36.2 Hz). MS (70 eV, EI): *m/z*: 288 [M^+], 259 [M−C_2H_5+], 231 [M−$COC_2H_5^+$]. IR (KBr): 1673 (CO) cm^{-1}. Anal. Calc. for $C_{14}H_{17}FeOP$: C, 58.36; H, 5.94. Found: C, 58.19; H, 6.13%.

5.2.6. 1,1-Di(4-hydroxyphenyl)-2-(dimethylphospholyl-cyclopentadienyl-iron)-but-1-ene (**9**)

$TiCl_4$ (10.0 ml, 9.1 mmol) was added dropwise to a suspension of zinc powder (1.0 g, 15.3 mmol) in 15 ml of THF at − 10°C. The dark grey mixture obtained was heated at reflux for 1.5 h. A solution of THF (7 ml) containing 4,4′-dihydroxybenzophenone (0.428 g, 2.0 mmol) and ketone **8** (0.452 g, 1.5 mmol) was added dropwise to the first solution and then the resulting mixture was heated for 2 h. After cooling to room temperature, the mixture was hydrolyzed with 20% HCl solution. After CH_2Cl_2 extraction and solvent removal, the crude product was chromatographed on silica gel column with CH_2Cl_2/acetone 10:1 as eluent to yield 9 as an orange solid (0.110 g, 16% yield). ^{1}H NMR (400 MHz, $CDCl_3$): δ 0.95 (t, 3H, J = 8 Hz, CH_3), 2.12 (s, 6H, CH_3), 2.48 (q, 2H, J = 8 Hz, CH_2), 3.33 (d, 2H, $J_{P–H}$ = 36 Hz, C_4H_2P), 3.96 (broad s, 2H, C_5H_4), 4.00 (broad s, 2H, C_5H_4), 4.93 (s, 1H, OH), 4.97 (s, 1H, OH), 6.68–7.06 (four d, J = 8 Hz, 8H, C_6H_4). ^{13}C NMR (100 MHz, acetone-d_6): δ 15.4 (CH_3), 16.0 ($2CH_3$), 28.0 (CH_2), 71.8 (2CH, C_5H_4), 72.8 (2CH, C_5H_4), 80.0 (d, $^2J_{P–C}$ = 60 Hz, C_4H_2P), 89.5 (C, C_5H_4), 95.5 (d, $^2J_{P–C}$ = 10 Hz, C_4H_2P), 115.3 (2 × $2CH_{arom}$), 130.5 ($2CH_{arom}$), 131.2 ($2CH_{arom}$), 135.8 (C), 137.2 (C), 137.6 (C), 138.1 (C), 153.9 (C), 154.0 (C). ^{31}P NMR

(161.9 MHz, $CDCl_3$): δ 79.1, $^2J_{P-H}$ = 36.3 Hz. MS (70 eV, EI): *m*/*z*: 470 [M^+]. IR (KBr): 3430 (OH), 1604 (C=C) cm^{-1}.

5.2.7. General procedure for formation of diphenols (**10**–**12**)

Titanium tetrachloride (0.7 ml, 6.3 mmol) was added dropwise to a suspension of zinc powder (0.8 g, 12 mmol) in 15 ml of THF at 0 °C. The mixture obtained was heated at reflux for 2 h. A second solution was prepared by dissolving 4,4′-dihydroxybenzophenone (0.43 g, 2 mmol) and the corresponding ketones [10] (1 mmol) in 10 ml of THF. This latter solution was added dropwise to the first solution and then the reflux was continued for 2 h. After cooling to room temperature, the mixture was stirred with water and dichloromethane. The mixture was acidified with diluted hydrochloric acid and was decanted. The aqueous layer was extracted with dichloromethane and the combination of organic layers was dried on magnesium sulfate. After concentration under reduced pressure, the crude product was chromatographed on silica gel plates with dichloromethane as eluent to give pure **10**–**12**.

5.2.8. 1,1-Di(4-hydroxyphenyl)-2-ruthenocenylbut-1-ene (**10**)

Yield 96%. Mp, 236 °C (ethanol). ^{1}H NMR (200 MHz, DMSO-d_6): δ 0.95 (t, *J* = 7.3 Hz, 3H, CH_3), 2.26 (q, *J* = 7.3 Hz, 2H, CH_2), 4.22 (s, 2H, C_5H_4), 4.39 (s, 2H, C_5H_4), 4.51 (s, 5H, Cp), 6.59 (d, *J* = 8.4 Hz, 2H, H_{arom}), 6.68 (d, *J* = 8.4 Hz, 2H, H_{arom}), 6.77 (d, *J* = 8.4 Hz, 2H, H_{arom}), 6.90 (d, *J* = 8.4 Hz, 2H, H_{arom}), 9.23 (s, 1H, OH), 9.28 (s, 1H, OH). ^{13}C NMR (50 MHz, DMSO-d6): δ 16.3 (CH_3), 29.4 (CH_2), 70.5 (2CH C_5H_4), 71.9 (5CH Cp), 72.4 (2CH C_5H_4), 92.8 (C C_5H_4), 115.7 (2CH_{arom}), 115.8 (2CH_{arom}), 130.7 (2CH_{arom}), 131.3 (2CH_{arom}), 135.0 (C), 135.9 (C), 136.2 (C), 138.7 (C), 156.4 (C), 156.5 (C). IR: 3428 (OH), 2964, 2928, 2872 (CH_3,CH_2) cm^{-1}. HRMS (CI): *m*/*z*: [$C_{26}H_{25}O_2Ru$: MH^+] calcd: 471.0905, found: 471.0894. Anal. Calc. for $C_{26}H_{24}O_2Ru$: C, 66.51; H, 5.15. Found: C, 66.39; H, 4.97%.

5.2.9. 1,1-Di(4-hydroxyphenyl)-2-cyrhetrenylbut-1-ene (**11**)

Yield 86%. Mp 81–83 °C (diethyl ether/pentane). ^{1}H NMR (200 MHz, acetone-d_6): δ 0.99 (t, *J* = 7.5 Hz, 3H, CH_3), 2.20 (q, *J* = 7.5 Hz, 2H, CH_2), 5.19 (t, *J* = 2.3 Hz, 2H, C_5H_4), 5.30 (t, *J* = 2.3 Hz, 2H, C_5H_4), 6.68 (d, *J* = 8.7 Hz, 2H, H_{arom}), 6.73 (d, *J* = 8.7 Hz, 2H, H_{arom}), 6.87 (d, *J* = 8.7 Hz, 2H, H_{arom}), 6.92 (d, *J* = 8.7 Hz, 2H, H_{arom}), 8.25 (s, 1H, OH), 8.29 (s, 1H, OH). ^{13}C NMR (50 MHz, acetone-d_6): δ 15.6 (CH_3), 29.7 (CH_2), 84.3 (2CH C_5H_4), 87.1 (2CH C_5H_4), 110.4 (C C_5H_4), 116.0 (2CH_{arom}), 116.2 (2CH_{arom}), 130.8 (2CH_{arom}), 131.4 (2CH_{arom}), 135.5 (C), 135.8 (C), 143.9 (C), 153.8 (C), 157.2 (C), 157.4 (C), 196.1 (3CO). IR: 3434 (OH), 2970, 2933, 2871 (CH_3,CH_2), 2016, 1916 (CO) cm^{-1}. HRMS (CI): *m*/*z*: [$C_{24}H_{20}O_5Re$: MH^+] calcd: 575.0869, found: 575.0869. Anal. Calc. for $C_{24}H_{19}O_5Re$ + 1/2H_2O: C, 49.48; H, 3.46. Found: C, 49.44; H, 3.62.

5.2.10. 1,1-Di(4-hydroxyphenyl)-2-cymantrenylbut-1-ene (**12**)

Yield 96%. Mp 88 °C (diethyl ether/pentane). ^{1}H NMR (200 MHz, $CDCl_3$): δ 1.04 (t, J = 7.5 Hz, 3H, CH_3), 2.29 (q, J = 7.5 Hz, 2H, CH_2), 4.47 (s, 2H, C_5H_4), 4.54 (s, 2H, C_5H_4), 4.81 (s, 1H, OH), 4.83 (s, 1H, OH), 6.73 (d, J = 8.4 Hz, 2H, H_{arom}), 6.77 (d, J = 8.4 Hz, 2H, H_{arom}), 6.95 (d, J = 8.4 Hz, 2H, H_{arom}), 7.04 (d, J = 8.4 Hz, 2H, H_{arom}). ^{13}C NMR (50 MHz, acetone-d_6): δ 15.5 (CH_3), 28.8 (CH_2), 82.6 (2CH, C_5H_4), 85.5 (2CH, C_5H_4), 106.7 (C C_5H_4), 116.0 ($2CH_{arom}$), 116.2 ($2CH_{arom}$), 130.9 ($2CH_{arom}$), 131.4 (C), 131.6 ($2CH_{arom}$), 135.8 (C), 136.0 (C), 144.0 (C), 157.2 (C), 157.4 (C), 206.1 (3CO). IR: 3447 (OH), 2970, 2932, 2871 (CH_3,CH_2), 2014, 1926 (CO) cm^{-1}. HRMS (CI): m/z: [$C_{24}H_{20}O_5Mn$: MH^+] calcd: 443.0691, found: 443.0682.

5.3. Biochemistry conditions

5.3.1. Materials

Stock solutions (1×10^{-3} M) of the compounds to be tested were prepared in DMSO and were kept at 4 °C in the dark; under these conditions they are stable at least two months. Serial dilutions in DMSO were prepared just prior to use. Dulbecco's modified eagle medium (DMEM) was purchased from Gibco BRL, fetal calf serum from Dutscher, Brumath, France, glutamine, estradiol and protamine sulfate were from Sigma. MCF7 and MDA-MB231 cells were from the Human Tumor Cell Bank. Sheep uteri weighing approximately 7 g were obtained from the slaughterhouse at Mantes-la-Jolie, France. They were immediately frozen and kept in liquid nitrogen prior to use.

5.3.2. Determination of the relative binding affinity (RBA) of the compounds for ERα and ERβ

RBA values were measured on ERα from lamb uterine cytosol and on ERβ purchased from Pan Vera (Madison, WI, USA). Sheep uterine cytosol prepared in buffer A (0.05 M Tris–HCL, 0.25 M sucrose, 0.1% β-mercaptoethanol, pH 7.4 at 25 °C) as described previously [5] was used as a source of ERα. For ERβ, 10 μl of the solution containing 3500 pmol/ml were added to 16 ml of buffer B (10% glycerol, 50 mM Bis–Tris–propane pH = 9, 400 mM KCl, 2 mM DTT, 1 mM EDTA, 0.1% BSA) in a silanized flask. Aliquots (200 μl) of ERα in glass tubes or ERβ in polypropylene tubes were incubated for 3 h at 0 °C with [6,7-^{3}H]-estradiol (2×10^{-9} M, specific activity 1.62 TBq/mmol, NEN Life Science, Boston MA) in the

presence of nine concentrations of the hormones to be tested. At the end of the incubation period, the free and bound fractions of the tracer were separated by protamine sulfate precipitation. The percentage reduction in binding of [^{3}H]-estradiol (Y) was calculated using the logit transformation of Y (logit$Y$: $\ln[y/1 - Y]$ versus the log of the mass of the competing steroid. The concentration of unlabeled steroid required to displace 50% of the bound [^{3}H]-estradiol was calculated for each steroid tested, and the results expressed as RBA. The RBA value of estradiol is by definition equal to 100%.

5.3.3. Measurement of octanol/water partition coefficient (log $P_{o/w}$) of the compounds

The log $P_{o/w}$ values of the compounds were determined by reverse-phase HPLC on a C-8 column (nucleosil 5.C8, from Macherey Nagel, France) according to the method previously described by Minick [31] and Pomper [32]. Measurement of the chromatographic capacity factors (k') for each compound was done at various concentrations in the range 85–60% methanol (containing 0.25% octanol) and an aqueous phase consisting of 0.15% *n*-decylamine in 0.02 M MOPS (3-morpholinopropanesulfonic acid) buffer pH 7.4 (prepared in 1-octanol-saturated water). These capacity factors (k') are extrapolated to 100% of the aqueous component given the value of k'_w.log $P_{o/w}$ (y) is then obtained by the formula: $\log P_{o/w} = 0.13418+0.98452\times\log k'_w$.

5.3.4. Culture conditions

Cells were maintained in monolayer in DMEM with phenol red (Gibco BRL) supplemented with 8-9% fetal calf serum (Gibco BRL) and glutamine 2 mM (Sigma) at 37 °C in a 5% CO_2 air humidified incubator. For proliferation assays, cells were plated in 1 ml of DMEM medium with or without phenol red, supplemented with 10% decomplemented and hormone-depleted fetal calf serum and 2 mM glutamine and incubated. The following day (D0) 1 ml of the same medium containing the compounds to be tested was added to the plates (final volumes of DMSO: 0.1%; four wells for each condition, one plate per day). After 3 days (D3) the incubation medium was removed and fresh medium containing the compounds was added. After 6 days (D6) the total protein content of the plate was analyzed by methylene blue staining as follows. Cell monolayers were fixed for 1 h in methanol, stained for 1 h with methylene blue (1 mg/ml) in PBS, then washed thoroughly with water. One ml of HCl (0.1 M) was then added and the absorbance of each well was measured at 620 nm with a Biorad spectrophotometer. The results are expressed as the percentage of proteins versus the control.

5.4. Electrochemistry conditions

Linear sweep cyclic voltamograms were obtained utilizing an Autolab PGStat20 potentiostat, driven by GPES software [33], a platinum wire counterelectrode, a 500 μM platinum disc working electrode, and an aqueous standard calomel reference electrode. Analyte solutions were 1–2 mM in MeOH with 0.1 M Bu_4NBF_4 supporting electrolyte. The system was not controlled for temperature, water, or oxygen.

Acknowledgements

We thank E. Salomon, A. Cordaville and M.A. Plamont for technical assistance. E.A.H. thanks the NSF (Grant no. E0302042) for financial support and Professor Christian Amatore for use of his electrochemistry equipment and helpful discussions.

References

[1] M.M. Buckley, K.L. Goa, Drugs 37 (1989) 451–490.

[2] A. Howell, A.M. Wardley, Endocrine-Related Cancer 12 (2005) S9–S16, and references cited therein.

[3] (a) P. Köpf-Maier, H. Köpf, Chem. Rev. 87 (1987) 1137–1152; (b) P. Köpf-Maier, H. Köpf, E.W. Neuse, Angew. Chem., Int. Ed. Engl. 23 (1984) 456–457.

[4] A. Vessières, S. Top, W. Beck, E.A. Hillard, G. Jaouen, Dalton Trans. (2006) 529–541.

[5] S. Top, A. Vessières, G. Leclercq, J. Quivy, J. Tang, J. Vaissermann, M. Huché, G. Jaouen, Chem. Eur. J. 9 (2003) 5223–5236.

[6] A. Vessières, S. Top, P. Pigeon, E.A. Hillard, L. Boubeker, D. Spera, G. Jaouen, J. Med. Chem. 48 (2005) 3937–3940.

[7] E.A. Hillard, A. Vessières, L. Thouin, G. Jaouen, C. Amatore, Angew. Chem., Int. Ed. 45 (2006) 285–290.

[8] A.S. Abd-El-Aziz, S. Bernardin, Coord. Chem. Rev. 203 (2000) 219–267.

[9] K. Kowalski, A. Vessières, S. Top, G. Jaouen, J. Zakrzewksi, Tetrahedron Lett. 44 (2003) 2749–2751.

[10] (a) Ruthenium: P. Pigeon, S. Top, A. Vessières, M. Huché, E.A. Hillard, E. Salomon, G. Jaouen, J. Med. Chem. 48 (2005) 2814–2820; (b) Rhenium: S. Top, A. Vessières, P. Pigeon, M.N. Rager, M. Huché, E. Salomon, C. Cabestaing, J. Vaissermann, G. Jaouen, Chem. Bio. Chem 5 (2004) 1104–1113; (c) Manganese: S. Top, E.B. Kaloun, A. Vessières, I. Laïos, G. Leclercq, G. Jaouen, J. Organomet. Chem. 643-644 (2002) 350–356.

[11] A. Rivas, M. Lacroix, F. Olea-Serrano, I. Laïos, G. Leclercq, N. Olea, J. Steroid Biochem. Mol. Biol. 82 (2002) 45–53.

[12] A.K. Shiau, D. Barstad, D.P.M. Loria, L. Cheng, P.J. Kushner, et al., Cell 95 (1998) 927–937.

[13] A.K. Shiau, D. Barstad, J.T. Radek, M.J. Meyers, K.W. Nettels, B.S. Katztenellenbogen, J.A. Katzenellenbogen, D.A. Agard, G.L. Greene, Nat. Struct. Biol. 9 (2002) 359–364.

[14] R.N. Hanson, E. Napolitano, R. Fiaschi, J. Med. Chem. 41 (1998) 4686–4692.

[15] Compound **9** did not give any signal in the CV.

[16] M.G. Hill, W.M. Lamanna, K.R. Mann, Inorg. Chem. 30 (1991) 4687–4690.

[17] C.P. Horwitz, N.Y. Suhu, G.D. Dailey, J. Electroanal. Chem. 324 (1992) 79–91.

[18] (a) D. Osella, M. Ferrali, P. Zanello, F. Laschi, M. Fontani, C. Nervi, G. Cavigiolio, Inorg. Chim. Acta 306 (2000) 42–48; (b) G. Tabbi, C. Cassino, G. Cavigiolio, D. Colangelo, A. Ghiglia, I. Viano, D. Osella, J. Med. Chem. 45 (2002) 5786–5796; (c) H. Tamura, M. Miwa, Chem. Let. 11 (1997) 1177–1178.

[19] (a) M.M. Marques, F.A. Beland, Carcinogenesis 18 (1997) 1949–1954; (b) P.W. Fan, F. Zhang, J.L. Bolton, Chem. Res. Toxicol. 13 (2000) 45–52.

[20] D. Chong, A. Nafady, P.J. Costa, M.J. Calhorda, W.E. Geiger, J. Am. Chem. Soc. 127 (2005) 15676–15677.

[21] A. Kallio, A. Zheng, J. Dahllund, K.M. Heiskanen, P. Härkönen, Apoptosis 10 (2005) 1395–1410.

[22] Y.S. Lee, Arch. Pharm. Res. 10 (2005) 1183–1189.

[23] M.A. Jakupec, M. Galanski, B.K. Keppler, Rev. Physiol. Biochem. Pharmacol. 146 (2003) 1–53.

[24] F. Wang, A. Habtermaram, E.P.L. van der Geer, R. Fernandez, M. Melchart, R. Deeth, R. Aird, S. Guichard, F.P.A. Fabbiani, P. Lozano-Casal, I.D.H. Oswald, D.I. Jodrell, S. Parsons, P.J. Sadler, Proc. Natl. Acad. Sci. USA 102 (2005) 18269–18274.

[25] (a) S. Kapitza, M. Pongratz, M.A. Jakupec, P. Heffeter, W. Berger, L. Lackinger, B.K. Keppler, B. Marian, J. Cancer Res. Clin. Oncol. 131 (2005) 101–110; (b) S. Kapitza, M.A. Jakupec, M. Uhl, B.K. Keppler, B. Marian Cancer Lett. 226 (2005) 115–121.

[26] (a) M.A. Jakupec, B.K. Keppler, Curr. Top. Med. Chem. 4 (2004) 1575–1583; (b) M.A. Jakupec, B.K. Keppler, Met. Ions Biol. Systems 42 (2004) 425–462.

[27] (a) G. Sava, S. Zorzet, C. Turrin, F. Vita, M. Soranzo, G. Zabucchi, M. Cocchietto, A. Bergamo, S. DiGiovine, G. Pezzoni, L. Sartor, S. Garbisa, Clin. Cancer Res. 9 (2003) 1898–1905; (b) J.M. Rademaker-Lakhai, D. van den Bongard, D. Pluim, J.H. Beijnen, J.H. Schellens, Clin. Cancer Res. 10 (2004) 3717–3727.

[28] (a) C. Scolaro, A. Bergamo, L. Brescacin, R. Delfino, M. Cocchietto, G. Laurenczy, T.J. Geldbach, G. Sava, P.J. Dyson, J. Med. Chem. 48 (2005) 4161–4171; (b) A. Dorcier, P.J. Dyson, C. Gossens, U. Rothlisberger, R. Scopelliti, I. Tavernelli, Organometallics 24 (2005) 2114–2123; (c) C. Scolaro, T.J. Geldbach, S. Rochat, A. Dorcier, S. Gossens, A. Bergamo, M. Cocchietto, I. Tavernelli, G. Sava, U. Rothlisberger, P.J. Dyson, Organometallics 25 (2006) 756–765; (d) B. Serli, E. Zangrando, T. Gianferrara, C. Scolaro, P.J. Dyson, A. Bergamo, E. Alessio, Eur. J. Inorg. Chem. (2005) 3423–3434.

[29] Wavefunction Society, 18401 Von Karman Avenue, Irvine, CA 92612, USA.

[30] L. Schwink, P. Knochel, T. Eberle, J. Okuda, Organometallics 17(1998) 7–9.

[31] D.J. Minick, J.H. Frenz, M.A. Patrick, D.A. Brent, J. Med. Chem. 31 (1988) 1923–1933.

[32] M.G. Pomper, H. VanBrocklin, A.M. Thieme, R.D. Thomas, D.O. Kiesewetter, et al., J. Med. Chem. 33 (1990) 3143–3155.

[33] General Purpose Electrochemical System, Version 4.8, EcoChemie B.V., Ultrect, The Netherlands.